THE ASTRONOMICAL JOURNAL VOLUME 106, NUMBER 5 NOVEMBER 1993

YOUNG OPEN CLUSTERS AS PROBES OF THE STAR-FORMATION PROCESS. II. MASS AND LUMINOSITY FUNCTIONS OF YOUNG OPEN CLUSTERS

RANDY L. PHELPS[1,2]

Phillips Laboratory, Optical Environment Division, Backgrounds Branch (GPOB), 29 Randolph Road, Hanscom Air Force Base, Massachusetts 01731-3010
Electronic mail: phelps@buast5.bu.edu

KENNETH A. JANES

Department of Astronomy, Boston University, Boston, Massachusetts 02215
Electronic mail: janes@buasta.bitnet

Received 1993 March 10; revised 1993 July 13

ABSTRACT

This paper is the second in a series devoted to the use of young, optically revealed open clusters as probes of the star-formation process. The first paper in the series [Phelps & Janes, ApJS (1993) (in press)] presented the dataset used for the study, and discussed some of the results from the survey of 23 open clusters in the Cassipoeia region of the Perseus spiral arm of our Galaxy. This paper presents an analysis of the stellar content of a subset of the clusters, including determinations of the luminosity and mass functions of 8 of the clusters to $\sim 1\mathcal{M}_\odot$. The slope of the average mass function Γ is found to be -1.40 ± 0.13 over the mass range $1.4 < \mathcal{M}/\mathcal{M}_\odot < 7.9$. Significant variations from this average value are found for two of the clusters, NGC 581 and NGC 663. Possible structure in the mass functions is discussed, as is the degree to which the IMF is universal, or merely an average of many IMFs that differ substantially on the local level.

1. INTRODUCTION

To fully understand star formation it is important to know just what the end result of the process is. In particular, it is important to understand how predictable the star-formation process is, and whether or not the same frequency distribution of stellar masses will arise from the fragmentation of molecular clouds. Another important question to address is whether or not star-formation processes differ in various parts of the Galaxy. Among the more useful tools in addressing these questions is the initial mass function (IMF).

The IMF, $\xi(\log m)$, is defined to be the number of stars formed per logarithmic mass interval, where m is the stellar mass. The IMF is most often discussed in terms of the field star IMF, where field stars are defined to be stars in the solar neighborhood; "neighborhood," however, depends upon the stellar mass since higher mass stars are not found in the immediate solar vicinity. Random velocities of stars also imply that low mass stars, with long lifetimes, have wandered a significant distance within the Galactic disk during their lifetimes. Higher mass stars, with much shorter lifetimes, will still be found near their birthsites.

The complexity involved in determining the field star IMF is enormous, and the resulting IMF suffers from numerous uncertainties. Among the many problems one encounters are too many inadequately known quantities which go into the construction of the IMF (see Scalo 1986), assumptions of the spatial and temporal invariance of the IMF, the contribution of unresolved binaries, and the cloaking of higher mass stars by their dense molecular birthsites. In particular, for the $1\text{–}2\mathcal{M}_\odot$ mass range, the unknown details of the relative birthrate history of stars leads Scalo (1986) to state that "...(it is) impossible to accurately estimate the form of the (field star) IMF for masses $1 \leqslant \mathcal{M}_\odot \leqslant 2$."

Samples in which the IMF is most nearly realized are young star clusters, in which the majority of stars have not evolved off the main sequence (although a significant fraction may not yet have evolved onto the main sequence either).

Open clusters have many advantages over field stars for a determination of the IMF.

(1) All stars are at essentially the same distance, allowing an accurate determination of the luminosity function to be made. The luminosity function can then be transformed into a mass function using a suitable mass–luminosity relation.

(2) If the range of formation times of the stars is less than the cluster age, then the observed luminosity function is directly transformable into the IMF below the main-sequence turnoff.

(3) Since the ages of clusters can be determined, unlike for field stars, one need not assume a time independent IMF.

(4) Cluster stars are all formed in the same region of space, unlike field stars with masses $\leqslant 2\mathcal{M}_\odot$, most of which move a significant distance from their birthsites during their lifetimes.

[1]Visiting Astronomer, Kitt Peak National Observatory, which is operated by the Association of Universities for Research in Astronomy, Inc., under contract with the National Science Foundation.
[2]National Research Council Associate.

 0004-6256/93/106(5)/1870/15/$0.90

(5) The form of the IMF from 1 to $2\mathcal{M}_\odot$ can be directly determined since the ages of the stars are known and birthrate corrections are not necessary.

There are, however, several complications in using young open clusters for the determination of the IMF.

(1) The relatively small number of stars means there are usually poor statistics involved in the determination of the IMF.

(2) Contamination by field stars makes membership determination of clusters difficult, especially since most young clusters are located very near the Galactic plane.

(3) Dynamical evolution may result in lower mass stars being found in more extended halos than the higher mass stars (cf. Lada *et al.* 1984). This results in the need for wider area coverage of the cluster which, however, greatly increases the proportion of field stars in the sample.

(4) If stars within clusters form with a spread in formation times, evolutionary corrections may be needed.

Nevertheless, young open clusters can provide an important sample of stars from which to learn about the IMF, and hence about the star-formation process. Studying the IMF is important not only for understanding the star-formation process itself, but also for interpreting star-formation regions as a whole, as well as for understanding galactic evolution and starburst galaxies (e.g., Tinsley 1980), since it is the high mass stars which dominate the structure of the interstellar medium and the chemical evolution of a galaxy.

An early, and influential study of the luminosity functions of clusters was that of van den Bergh & Sher (1960), who determined the luminosity functions of 20 open clusters. They found variations in the luminosity functions, with an apparent turnover at fainter magnitudes, unlike that seen in the field star IMF. This result suggested the possibility that star formation differs in clusters compared to the field, a concept which has since come to be known as "Bimodal Star Formation" (cf. Mezger & Smith 1977; Larson 1986).

In recent years, luminosity and mass functions have been determined for a number of open clusters. In the optical, recent studies include NGC 3293 (Herbst & Miller 1983), NGC 2362 (Wilner & Lada 1991), Praesepe (Jones & Stauffer 1991), the Hyades (Reid 1992), and the Pleiades (Stauffer *et al.* 1991). The Stauffer *et al.* study of the Pleiades (age $\sim$80 Myr) reaches absolute magnitude ($M_V \sim 12.5$) and shows a rising luminosity function to the completeness level of $M_V = 10.5$, with a dip centered at $M_V \sim 7$. The Reid (1992) luminosity function for the Hyades is similar to that of the local field stars, reaching a maximum near $M_V \sim 12$. The luminosity function of Praesepe rises to the completeness limit of $M_V = 11$. The luminosity functions of both NGC 2362 and NGC 3293 (ages of $\sim$7 Myr) exhibit nearly identical dips in the luminosity functions at $M_V = 2$–3 (Wilner & Lada 1991). The NGC 2362 mass function rises to below $1\mathcal{M}_\odot$, although some disagreement exists as to whether or not the mass function follows the field star IMF (see Kroupa *et al.* 1992),

Numerous near-IR studies of embedded cluster luminosity functions have also been conducted. Lada *et al.* (1991) identified more than 100 OB stars in M17 with a mass function consistent with that of Salpeter (1955). Hodapp & Rayner (1991), based on the K-magnitude luminosity function, detected stars of 0.2–$0.5\mathcal{M}_\odot$ in the S106 cluster. Wilking *et al.* (1989) in their study of ρ Oph found evidence for a deficiency of intermediate mass objects in the cluster. The K-band luminosity function of the Trapezium (Zinnecker & McCaughrean 1991) shows a steady rise to $K \sim 12$, indicating that a substantial population of low mass stars is present in this cluster.

2. PROGRAM

In a previous paper (Phelps & Janes 1993, hereafter referred to as Paper I), we presented a photometric atlas of 23 open clusters in or near the Cassiopeia region of the Perseus spiral arm, and presented initial results from that survey. Several of those clusters are ideal targets for a study of the IMF, in particular, for the mass range $1 < \mathcal{M}_\odot < 2$. The small angular sizes of the clusters, coupled with the faint limiting magnitude ($V \sim 21$) obtained in this study, allows wide field photometry of most of these clusters to $\sim 1\mathcal{M}_\odot$. With these data we can investigate possible structure in the mass functions, and probe the degree to which the IMF is universal, or merely an average of many IMFs that differ substantially on the local level.

Since membership information from proper motion studies is not available for the majority of the cluster stars, and because field star contamination in the color–magnitude diagrams (CMDs) makes membership determination by photometric means difficult, it is necessary to obtain the luminosity (and hence mass) functions of the

TABLE 1. Clusters with measurable luminosity functions.

Name	α (1950)	δ (1950)	$(m-M)_V$	$(m-M)_0$	E($B-V$)	$R_{\rm Lynga}$ (′)	$R_{\rm full}$ (′)	$N_{\rm stars}$	Age (Myr)
NGC 663	01:42.6	61:00	14.73	12.25	0.80	7.0	4.4	400	12–25
NGC 659	01:40.8	60:27	14.65	12.70	0.63	2.5	2.3	60	22
Tr 1	01:32.3	61:02	13.99	12.10	0.61	1.5	2.6	100	27
NGC 581	01:29.9	60:27	13.51	12.15	0.44	2.5	4.6	···	10–22
NGC 457	01:15.9	58:04	13.92	12.40	0.49	10.0	6.2	600	7–19
NGC 436	01:12.5	58:33	14.10	12.55	0.50	2.5	2.3	200	42
NGC 103	00:22.5	61:04	14.61	12.90	0.55	2.5	3.9	300	20
NGC 7790	23:55.9	60:56	14.56	12.75	0.55	2.5	3.6	150	71

TABLE 2. Field regions.

Region	α(1950)	δ(1950)
Field region 1	01:19:11	57:31
Field region 2	01:08:16	58:12
Field region 3	01:16:51	58:40
Field region 4	01:10:47	59:01
NGC 663 field	01:46:02	61:01

clusters by statistical means. To construct a cluster luminosity function, photometry of a nearby field region with the same stellar background distribution as the cluster frame is required. Histograms, as a function of magnitude, are constructed for the field region frame and the cluster frame (which has a contribution from the noncluster background). If the background star distribution in the CMD is the same in both the cluster and field frames, then subtracting the histogram of the magnitudes of the field frame from the cluster frame should result in the net distribution of cluster stars as a function of magnitude. If the cluster distance is known, this distribution of magnitudes (the V magnitude, for example) can be converted to a distribution in absolute magnitude, which is equivalent to a luminosity function for the cluster. Once the luminosity function has been constructed, the transformation to the mass function is done by the use of an appropriate mass–luminosity relation.

2.1 Cluster Data

While data on 23 clusters have been obtained (Paper I), not all of the clusters are suitable for determination of luminosity functions. Field region data, which is essential for the determination of the luminosity function, was not obtained for some of the clusters (see Sec. 2.2). Clusters for which suitable field region data are available are listed in Table 1. This table also summarizes cluster properties, including the radii from the Lyngå (1987) catalogue, and the apparent and true distance moduli (columns 4 and 5), reddening (column 6), radii (column 8), number of cluster stars (column 9), and ages (column 10) derived in Paper I.

For a few clusters, even though there is no field region data available, the cluster/field star contrast is sufficiently high that some information on stellar content can be obtained. For example NGC 654, for which no field region data are available, appears to be in front of a molecular cloud, eliminating most of the background stars from view, making a qualitative assessment of its stellar content possible.

Even for those clusters where appropriate field region data are available, the photometry does not always cover the entire area of the clusters. This is especially true for NGC 457 and NGC 663, where bright stars forced the omission of certain regions of the clusters in the CCD mosaics (see the photometric maps of Paper I). The CCD images of NGC 436, NGC 659, and Tr 1 cover the apparent sizes of the clusters, but would not cover a large enough area to detect low mass stars in possible halos

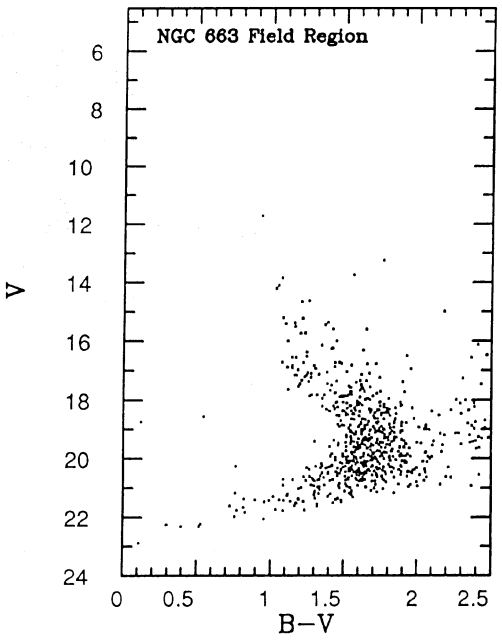

FIG. 1. CMD for the NGC 663 field region.

around the clusters. The larger format chip used to observe NGC 103 and NGC 7790 covers a substantial area and would cover at least a portion of any halo. As pointed out by Wilner & Lada (1991), however, little useful information can be obtained in the outer regions, where field stars statistically overwhelm faint cluster stars, unless an independent way of assigning cluster membership is available.

2.2 Field Region Data

In total, five field regions are available for use in the construction of cluster luminosity functions. The locations of these regions are listed in Table 2. The CMD of NGC 663 (see Paper I) indicates that NGC 663 is in front of a molecular cloud, since few field stars are seen in the CMD. The field region used with NGC 663 is presented in Fig. 1, and shows the same overall appearance as the parts of the NGC 663 CMD that are not associated with the cluster main sequence. This suggests that the field region of Fig. 1 is a good representation of the field star background in the CMD of NGC 663.

The other four field regions are presented in Figs. 2(a)–2(d), and show a characteristic wedge-shape which is seen in many of the cluster CMDs (see Paper I). The availability of CMDs for both the field regions and the clusters allows appropriate field regions to be selected, even though a cluster may be located a large distance on the sky from the selected field region. Without both the cluster and field region CMDs, it is difficult to assess the appropriateness of the field region when constructing a luminosity function.

2.3 Constructing Luminosity Functions

Histograms of the numbers of stars, at 1 mag intervals in V, were constructed for the cluster regions and the field

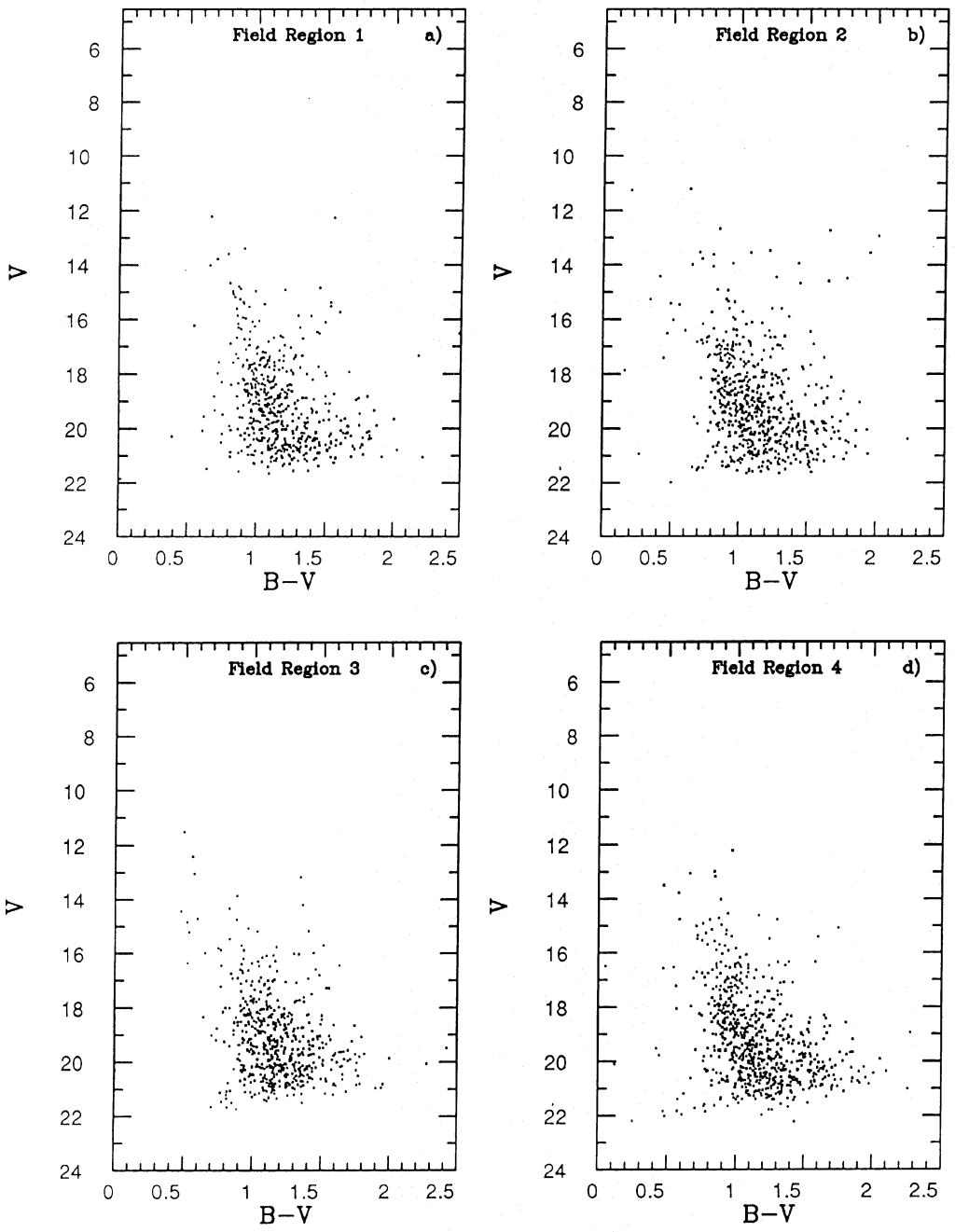

FIG. 2. (a)–(d) CMDs for two of the four field regions used in the construction of luminosity functions (except for NGC 663).

regions. Histograms for the field regions used for all of the clusters, except for NGC 663, are shown in Fig. 3. One mag intervals were selected to include enough stars per magnitude bin for the best possible statistics in establishing the form and variations in the luminosity and mass functions. The large bin size also means that uncertainties in the distance moduli of the clusters, typically 0.1–0.15 mag, will not be a significant factor in the uncertainties in the luminosity functions. For each cluster, an appropriate field region histogram was subtracted from the cluster region histogram to obtain what is taken to be the apparent net cluster luminosity function, which is then converted to M_V with the derived apparent distance modulus of the cluster (Table 1). Several clusters were observed with a larger format CCD, or with mosaics of CCD fields and thus cover larger area on the sky than individual field regions. For these clusters, photometry for up to four individual field regions was combined to form an average field region, and scaled to the area covered by the cluster observations for the determination of the luminosity function.

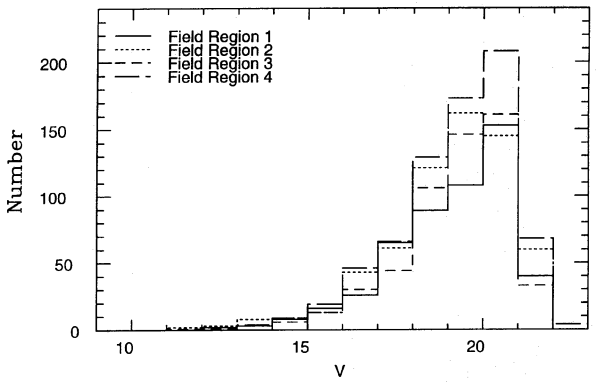

FIG. 3. Luminosity functions for the four field regions used to construct the cluster luminosity functions (except for NGC 663).

2.4 Uncertainties in the Luminosity Functions

Ideally one would have many field regions, completely surrounding each cluster, to reduce uncertainties in the derived luminosity functions that result from variations in the stellar distribution within the field regions. This, however, is not a practical approach in a large survey, and more distant field regions are sometimes used, resulting in potentially larger uncertainties; for despite the similar appearance of the CMDs of the field regions, differences do exist. The degree to which the individual field regions differ sets the limit to which the overall luminosity functions of the clusters are reliable.

In order to establish the uncertainties in the cluster luminosity functions as a result of random differences in field regions, luminosity fuctions for each of the field regions were constructed, at 1 mag intervals, and differences between all pairings, at each magnitude level, were obtained. This results in an estimate, at each magnitude level, of the uncertainties in the luminosity function of a cluster, with the same observed area, which arise as a result of field region variations. The average variations in the luminosity functions (Δn) per square arcmin, in each magnitude bin are listed in Table 3, along with the average number of stars found in each bin. These errors must be scaled to the appropriate area over which the cluster was observed, and are taken to be the uncertainties in the cluster luminosity functions, at each magnitude, in the following sections. The dispersion is quite large, and these values should be taken as minimum estimates of the uncertainties in the luminosity functions. They are, however, generally considerably larger, and more realistic, than Poisson uncertainties.

TABLE 3. Mean field region differences.

Mag	Δn stars/(arcmin)^2	Dispersion stars/(arcmin)^2	n stars/(arcmin)^2
9.5	0.000	0.000	0.000
10.5	0.000	0.000	0.000
11.5	0.023	0.016	0.017
12.5	0.023	0.016	0.046
13.5	0.056	0.056	0.104
14.5	0.046	0.023	0.185
15.5	0.069	0.049	0.353
16.5	0.324	0.141	0.840
17.5	0.301	0.227	1.367
18.5	0.588	0.243	2.577
19.5	0.927	0.459	3.411
20.5	0.621	0.521	3.863
21.5	0.524	0.246	1.164
22.5	0.037	0.051	0.000

2.5 Completeness

Digital analysis techniques allow the completeness of the photometry to be checked. The photometry software used in this study is the SPS package (Janes & Heasley 1993). The SPS photometry reduction program includes routines to randomly add artificial stars of a specified magnitude to images, which can then be identified and measured by standard techniques. Since the number of artificial stars added to the frame is known, the number of stars retrieved gives an estimate of the completeness of the photometry at various magnitude levels. For details of the artificial star routine incorporated within SPS, the reader is referred to Janes & Heasley (1993).

For this program, a representative cluster (NGC 436) and field region (field region 2) were chosen for a completeness test in two colors (B and V). The photometric reduction to the standard system requires two colors (see Paper I), meaning that the V luminosity function is affected not only by completeness in the V image, but also the B image. Ideally completeness should be established for each individual image in both colors, for all clusters. Because of the large number of frames involved in the construction of the luminosity functions (56 frames) a comprehensive completeness analysis would be impractical. All cluster and field frames were obtained under similar circumstances so the two test fields provide a limit to which the luminosity fuctions are reliable.

For each of the two test fields (NGC 436 and field region 2), in both colors, approximately 25–30 artificial stars were randomly added to the images at 0.5 mag intervals, from 17.5 to 22.5 mag. At each of the 11 mag (with the exception of $V=22.5$ in the V images), the artificial star test was repeated 5 times to obtain a representative completeness at that magnitude. Completeness was ranked on a scale of 0–1, with 1 indicating all of the artificial stars were retrieved (i.e., 100% completeness). This resulted in 210 photometric reductions for the two test fields in the two colors. The results of the completeness test are shown in Table 4, which lists the magnitude for which completeness was checked in each image, and the average and standard deviation for the completeness at that magnitude.

For most of the clusters, the photometry is more than 90% complete to a B magnitude of $\sim$21 which, for a star with $(B-V)=1.5$, means that the luminosity functions will be nearly complete to $V\sim19.5$. Exposure times for the B images were intentionally longer to match the sensitivity of the V images. From Table 4, the V photometry is 97% complete at $V=19.5$ ($\sim$1.5–2 magnitudes above the sensitivity limit of the photometry). The field region photom-

TABLE 4. Completeness.

Frame	Mag	Completeness	σ	Frame	Mag	Completeness	σ
NGC 436 (V)	17.5	1.00	0.00	NGC 436 (B)	17.5	1.00	0.00
	18.0	1.00	0.00		18.0	1.00	0.00
	18.5	1.00	0.00		18.5	1.00	0.00
	19.0	0.94	0.02		19.0	1.00	0.00
	19.5	0.96	0.05		19.5	1.00	0.00
	20.0	0.97	0.03		20.0	0.95	0.02
	20.5	0.88	0.02		20.5	0.96	0.03
	21.0	0.82	0.05		21.0	0.97	0.03
	21.5	0.80	0.06		21.5	0.86	0.02
	22.0	0.57	0.12		22.0	0.81	0.03
	22.5	...	...		22.5	0.52	0.10
Field 2 (V)	17.5	1.00	0.00	Field 2 (B)	17.5	1.00	0.00
	18.0	1.00	0.00		18.0	1.00	0.00
	18.5	1.00	0.00		18.5	1.00	0.00
	19.0	0.93	0.01		19.0	1.00	0.00
	19.5	0.93	0.03		19.5	1.00	0.00
	20.0	0.91	0.03		20.0	1.00	0.00
	20.5	0.93	0.06		20.5	0.95	0.02
	21.0	0.91	0.04		21.0	0.95	0.01
	21.5	0.78	0.05		21.5	0.83	0.02
	22.0	0.35	0.11		22.0	0.73	0.09
	22.5	...	...		22.5	0.35	0.10

etry has greater than 90% completeness to ~21st mag in both B and V. It is estimated, therefore, that the luminosity functions of the clusters are complete to $V\sim 19$–19.5, with the absolute magnitudes and masses associated with this magnitude range dependent on the distance to the individual cluster. The photometry of NGC 581 and NGC 7790 is complete to only $V\sim 18$ (1.5–2 mag above the limit of the photometry) because of the shorter integration times used when obtaining the data. For NGC 103, the completeness level is substantially fainter due to the longer integration times for this cluster, with a completeness limit estimated to be $V\sim 20.5$ based on the $V=21.5$–22.0 limit of the photometry.

The completeness in the field region generally extends a magnitude or more fainter than in the cluster frames because of the lower level of crowding in the field region, so that at faint magnitudes the field shows an excess of stars over the cluster region (indicated by dashed lines in the luminosity functions). Interpretations of the data at the faint end of the luminosity function, beyond the completeness limit of the cluster frames, should be avoided.

2.6 Mass Functions

The conversion of the luminosity (M_V) functions to mass functions was through the mass–luminosity relation given in Table IV of Scalo (1986). This relation is derived from his extensive review of both observational and theoretical studies over a wide mass range. Uncertainties in the mass–luminosity relation result from numerous factors and are thoroughly discussed by Scalo (1986), but over the range of absolute magnitudes observed in this study ($-5<M_V<5$) the uncertainty in log (mass) is typically 0.1 (see Table III of Scalo 1986). Uncertainties in log(N), the log of the number of stars at a given log (mass), are scaled from the uncertainties derived from the luminosity functions (Sec. 2.4), with the Scalo (1986) mass–luminosity relation.

Power-law fits to the mass functions, using a linear least-squares fit, were made to the regions of the mass function where the photometry is complete (see Sec. 2.5) and the stars have not evolved off the main sequence. These regions are indicated by the solid lines in the mass function figures, with extrapolations of the power-law fit indicated by dashed lines. In many cases the extrapolations also fit the observed mass functions, indicating that the choice of regions to fit the power law were conservative.

2.7 Form of the IMF

An often used parameter in discussions of the IMF is the index of the mass function, defined as

$$\Gamma(m)=\left.\frac{\partial \log \xi(\log m)}{\partial \log m}\right|_m. \quad (1)$$

For a power-law mass spectrum (which has an index independent of mass), the widely quoted Salpeter (1955) field star IMF has an index (slope) of $\Gamma=-1.35$. The lognormal field star IMF of Miller & Scalo (1979) has an index of $\Gamma=-(1+\log m)$.

As discussed by Scalo (1986), the consideration of the IMF as a probability distribution means that gaps between masses in the CMD might be expected. The probability that a star has a mass greater than xm_l, where m_l is the mass at the lower portion of the main sequence gap, is x^{Γ} for a power-law IMF (see Scalo 1986, p. 12). The probability ($P_{\rm gap}$) of finding a gap between masses m_l and xm_l with N stars more massive than xm_l, if the masses of the consecutively formed stars are independent is, from Scalo (1986, p. 12)

$$P_{\rm gap}=x^{N\Gamma} \quad (2)$$

for a power-law mass spectrum. In at least three of the program clusters, Be 7, Be 62, and NGC 637, gaps are detected in the main sequence, that according to Eq. (2), are of low probability for occurring randomly.

3. RESULTS

The following section presents the luminosity and mass functions of the eight clusters for which appropriate field region data were available. The stellar contents of four other clusters, for which meaningful statements can be made, are also discussed. The stellar contents of the remaining clusters in this survey are difficult to determine, because of variable reddening, field star contamination, or poor contrast between the cluster and the field, so they are omitted from this discussion.

Gaps or dips in the cluster luminosity/mass functions are noted when they are detected although, within the uncertainties given by the error bars, their significance is often marginal. There is interest in possible structure within luminosity functions (cf. Stahler & Fletcher 1991; Wilner & Lada 1991), however, and identification of features, if they occur repeatedly at the same absolute magnitude/mass, may lead to a better understanding of the IMF.

The results of this analysis for individual clusters are discussed in the following sections, with a summary given in Table 6.

3.1 Berkeley 7

Field region data appropriate for the construction of the luminosity and mass fuctions of Be 7 (age 0–4 Myr) were not obtained. The CMD (see Paper I), however, shows a noticeable gap in the main sequence between $13<V<14(-1.5<M_V<-0.5)$, or $3.0<\mathcal{M}/\mathcal{M}_\odot<4.3$. The probability of finding a gap of a factor of 1.4 times in mass, with $N=4-6$ stars above the gap (the number depends on uncertain membership of the stars), and assuming a power law IMF with slope $\Gamma=-1.35$, is 0.07–0.16, using Eq. (2) (from Scalo 1986).

3.2 NGC 663

A nearby field frame was obtained for NGC 663 (age 12–25 Myr) allowing the luminosity function and IMF of the cluster to be determined. A field region near NGC 663 is crucial because the cluster appears to be located in front of a molecular cloud, resulting in few field stars in the CMD (see Paper I). The CMD for the NGC 663 field region is shown in Fig. 1, and has a similar distribution of stars as the field stars in the cluster CMD (Paper 1). The area observed in the NGC 663 field is 1.7 times greater than that observed in the single frame field region. After applying this scaling factor, the luminosity and mass functions of Fig. 4 result. The limiting magnitudes of the cluster frames and the field region are nearly identical, as seen in their respective CMDs.

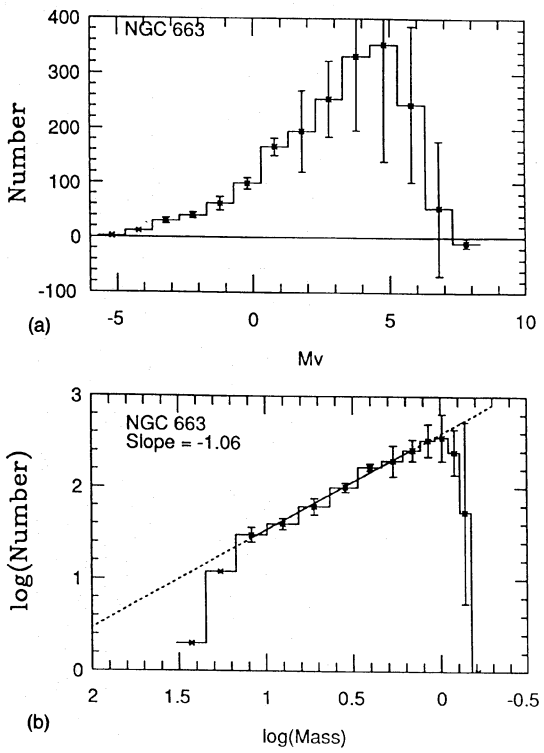

FIG. 4. (a) Luminosity function for NGC 663. (b) Mass function for NGC 663. Solid line indicates the region over which the least-squares fit was made, yielding a slope of -1.06 for the mass function.

The luminosity function continues to rise to $M_V=5$ and falls precipitously thereafter due to incompleteness in the photometry. With completeness becoming a problem for an apparent V magnitude of ~ 19 and fainter, the luminosity function is complete to $M_V\sim 4$, or a mass of $1.2\mathcal{M}_\odot$ ($\log\mathcal{M}=0.07$), with the stars brighter than $V\sim 12$ ($M_V=-3$), or more massive than $12\mathcal{M}_\odot$ ($\log\mathcal{M}=1.08$), having evolved off the main sequence. There is no apparent structure in the luminosity function to the level where the photometry is complete. A power-law fit to the unevolved, complete portion of the mass function (solid line) gives a slope of -1.06 ± 0.05.

The lack of field stars in the CMD of NGC 663, and the appearance of lower mass stars above the ZAMS (see Paper I), makes this cluster a prime target for future studies of PMS stars in young open clusters.

3.3 NGC 659

Field region 1 was used in the construction of the mass and luminosity functions of NGC 659 (age 22 Myr). Despite the large separation on the sky between the field region and the cluster, the distribution of field stars in the CMD of NGC 659 appears similar to that of the field region, suggesting that a reliable determination of the cluster luminosity function can be made. The areas observed for the cluster and field regions are equal, and comparison of the two fields results in the cluster luminosity function

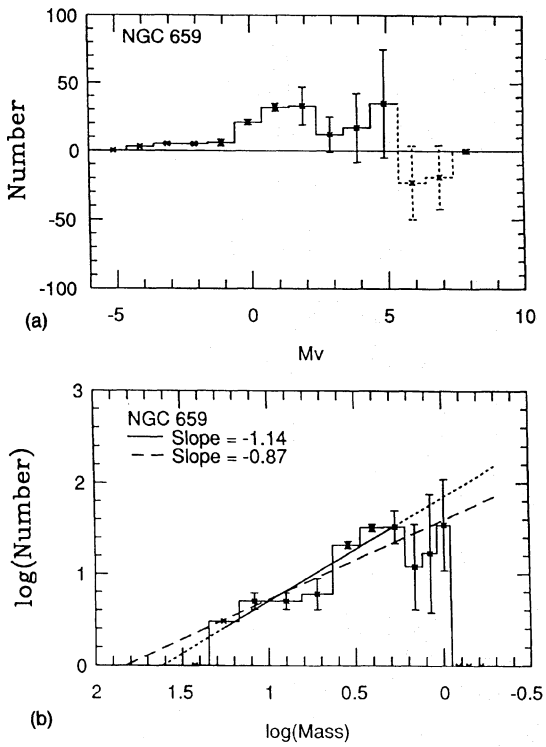

FIG. 5. (a) Luminosity function for NGC 659. Dashed line indicates the magnitude range where the field region photometry has greater completeness. (b) Mass function for NGC 659. Solid line indicates the region over which the least-squares fit was made, omitting the point in the "dip," yielding a slope of -1.14 for the mass function. Dashed line (long dashes) is the fit over the entire region where the photometry is complete.

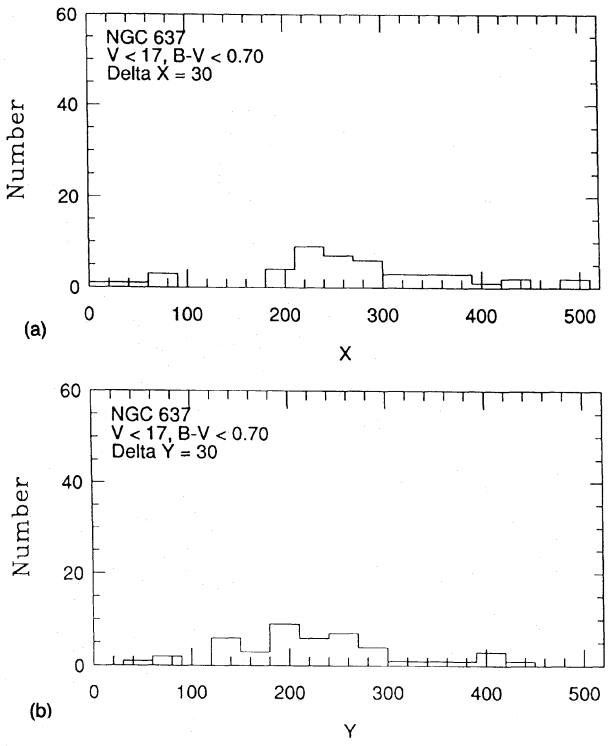

FIG. 6. Marginal distribution for stars with $V<17$ ($M_V<2.7$) in NGC 637.

of Fig. 5(a). The photometry of the cluster frame is complete to $V\sim19$–19.5, corresponding to $M_V\sim4$–4.5. A noticeable dip in the luminosity function occurs at $M_V\sim3$-4. The depression in the luminosity function is not, however, due to incompleteness since at $M_V\sim5$ the luminosity function rises again, and the photometry is most certainly not more incomplete at brighter magnitudes.

The mass function for NGC 659 is shown in Fig. 5(b). Based upon the completeness of the photometry, the mass function is complete down to $1.2\mathcal{M}_\odot$ ($\log\mathcal{M}=0.07$), with the stars brighter than $V\sim10.5$ ($M_V=-4$), or more massive than $18\mathcal{M}_\odot$($\log\mathcal{M}=1.40$), having evolved off the main sequence. A power law fit over the mass range $18<\mathcal{M}/\mathcal{M}_\odot<1.9$ gives a slope of -1.14 ± 0.17.

3.4 NGC 654

Field region data appropriate for the construction of a luminosity function for NGC 654 were not obtained, nor was the complete cluster observed due to bright stars in a portion of the cluster field. This cluster, like NGC 663, appears to be in front of a dense molecular cloud (see Paper I), reducing the number of field stars that would otherwise contaminate the CMD. A substantial number of low mass stars are visible in the CMD down to $V\sim20$ ($M_V\sim8$), with a strong concentration above the main sequence. The youth of the cluster (~25 Myr) means that stars with masses less than $\sim1\mathcal{M}_\odot$ ($M_V\sim5$ or $V\sim17$) would not yet have reached the main sequence (Stahler 1983) and would lie above it, as is seen in the CMD (Paper I). Since there are so few field stars in the CMD of NGC 654, this cluster is an ideal candidate for follow up studies of the IMF and the PMS content of young open clusters.

3.5 NGC 637

Appropriate field region data for NGC 637 (age 0–4 Myr) were not obtained. The CMD, however, shows a significant gap in the main sequence (Paper I) between $11<V<12(-3<M_V<-2)$, or $8<\mathcal{M}/\mathcal{M}_\odot<12$. The probability of finding a gap of a factor of 1.5 times in mass, with $N=7$ stars above the gap, and assuming a power-law IMF with slope $\Gamma=-1.35$, is 0.02 using Eq. (2) (from Scalo 1986).

The CMD (Paper I) shows an absence of a well-defined main sequence for $V>18$ ($M_V>3.7$). The youth of the cluster (4 Myr) implies that stars with masses less than $3\mathcal{M}_\odot$ ($M_V=0.5$, or $V\sim14.5$) are in their PMS stage of evolution (Stahler 1983) and should appear above the main sequence. Field star contamination in the CMD makes it difficult to establish the presence of a PMS population, however.

The marginal distribution, for all stars with $V<17$ ($M_V<2.7$) in the CMD (Paper 1), is shown in Fig. 6. A background of 1.0 field star per bin is found in the marginal distributions. Using this as a baseline resulting from

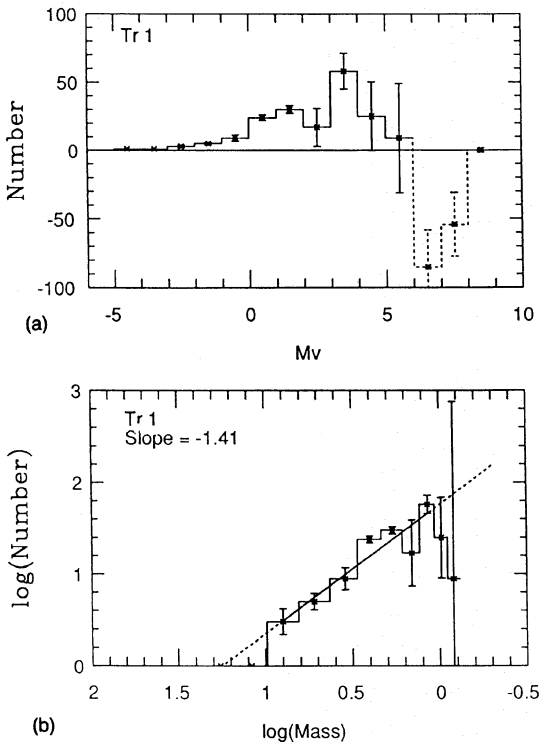

FIG. 7. (a) Luminosity function for Tr 1. Dashed line indicates the magnitude range where the field region photometry has greater completeness. (b) Mass function for Tr 1. Solid line indicates the region over which the least-squares fit was made, yielding a slope of −1.41 for the mass function.

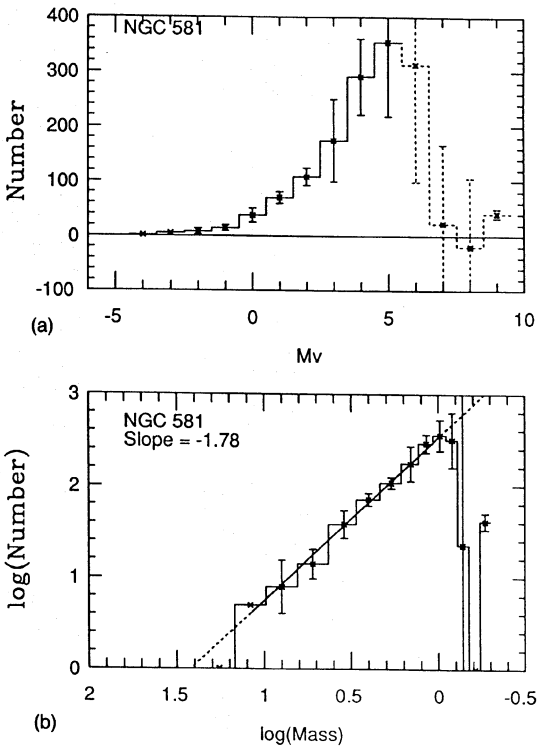

FIG. 8. (a) Luminosity function for NGC 581. Dashed line indicates the magnitude range where the field region photometry has greater completeness. (b) Mass function for NGC 581. Solid line indicates the region over which the least-squares fit was made, yielding a slope of −1.78 for the mass function.

field star contamination, the marginal distributions imply ~26 cluster stars with $V<17$ ($M_V<2.7$) compared with 55 ± 7 stars with $V<20$ ($M_V<5.7$) found from the cumulative distribution (see Paper I). The nearly equal number of stars with $M_V<2.7$ and $2.7<M_V<5.7$ is consistent with the ratio of the number of stars found over the same absolute magnitude range in NGC 663, with a mass function slope of ~-1.1. It is therefore likely that NGC 637 has a similar mass function, although an independent determination is required to test this conclusion.

3.6 Trumpler 1

Field region 2 was used to construct the luminosity function of Tr 1 (age 27 Myr). The apparent distance modulus of the cluster and the completeness limit of ~19 results in the luminosity function being complete to $M_V\sim5$. The luminosity function is shown in Fig. 7(a). An apparent dip in the luminosity function occurs at $M_V=2$–3.

The derived mass function for Tr 1 is shown in Fig. 7(b). The apparent dip in the luminosity function corresponds to the dip at $1.40\mathcal{M}_\odot$, or $\log\mathcal{M}=0.15$. A power-law fit to the mass function over the unevolved region where the photometry is complete ($1.2<\mathcal{M}/\mathcal{M}_\odot<7.9$, or $0.07<\log\mathcal{M}<0.90$), gives a slope of -1.41 ± 0.24.

3.7 NGC 581

Photometry of field regions 1, 2, 3, and 4 was combined, and scaled to the appropriate area to construct the luminosity function of NGC 581. As can be seen in the mosaic of images used to survey the cluster region (Paper I), the center frame suffers from greater incompleteness than the others due to the shorter exposure times necessitated by the brighter stars in the region. The completeness of this central frame is estimated to be $V\sim18.5$, corresponding to $M_V\sim5$. The luminosity function [Fig. 8(a)] steadily rises to this magnitude, with no apparent structure visible.

A power-law fit over the mass range in which the photometry is complete ($V\sim17.5$–18.0) and the stars are relatively unevolved ($1.2<\mathcal{M}/\mathcal{M}_\odot<12$, or $0.07<\log\mathcal{M}<1.08$) gives a slope of -1.78 ± 0.05 for the mass function. No significant deviation from the power law is seen, although a slight deviation at $\log\mathcal{M}=0.72$ ($5.2\mathcal{M}_\odot$), or $M_V\sim-1$ ($V\sim12.5$) corresponds to a visible gap in the main sequence of NGC 581 at $V\sim13$ in the CMD (Paper I).

3.8 NGC 457

Photometry of field regions 1, 2, 3, and 4 was combined and scaled to the observed area of NGC 457 to obtain its

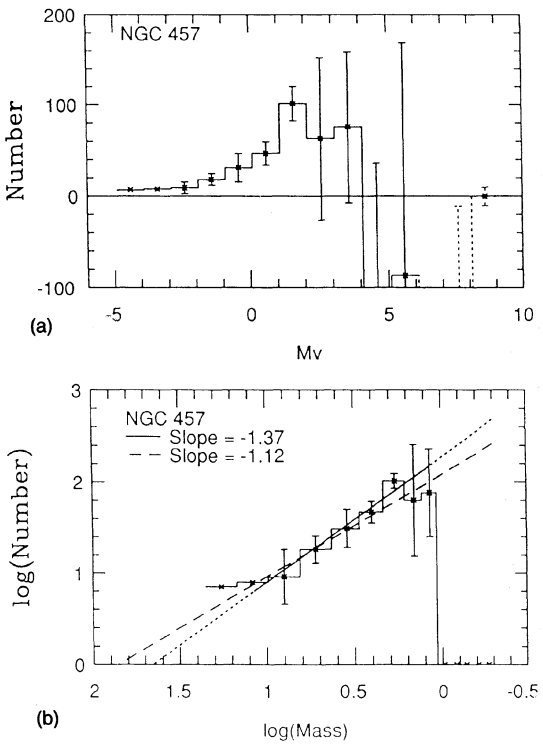

FIG. 9. (a) Luminosity function for NGC 457. Dashed line indicates the magnitude range where the field region photometry has greater completeness. (b) Mass function for NGC 457. Solid line indicates the region over which the least-squares fit was made, omitting the point in the dip, yielding a slope of -1.37 for the mass function. Dashed line (long dashes) is the fit over the entire region where the photometry is complete.

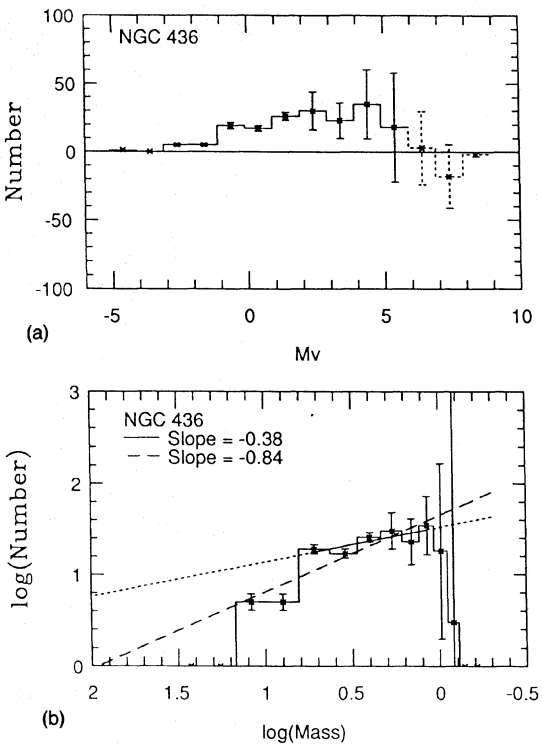

FIG. 10. (a) Luminosity function for NGC 436. Dashed line indicates the magnitude range where the field region photometry has greater completeness. (b) Mass function for NGC 436. Solid line indicates the region over which the least-squares fit was made, yielding a slope of -0.38 for the mass function. Dashed line (long dashes) is the fit extended to the higher mass stars, although these stars are likely to be evolved.

luminosity function. The apparent distance modulus of NGC 457, $(m-M)_V=13.92$, coupled with a completeness limit of $V\sim 19$–19.5 in the photometry, results in a luminosity function complete to $M_V\sim 5$–5.5 (Fig. 9). A noticeable dip at $M_V=2.5$, followed by a sharp break at $M_V=4$, occurs in the luminosity function, well above the completeness limit of $M_V=5$–5.5. Although the statistical uncertainties are large, it is difficult to explain this break in the luminosity and mass functions as being due to anything other than a deficiency of low mass stars. It is difficult to characterize the dip at $M_V=2.5$, given the sharp drop at fainter magnitudes, although dips are seen in other luminosity functions at this same absolute magnitude.

A power-law fit to the mass function over the range ($1.2<\mathcal{M}/\mathcal{M}_\odot<12$, or $0.07<\log\mathcal{M}<1.08$) gives a slope of -1.12 ± 0.13. This slope is heavily influenced by the dip and sharp cutoff in the mass function for masses less than $1.9\mathcal{M}_\odot(\log\mathcal{M}=0.27)$. A power law fit to the mass range ($1.9<\mathcal{M}/\mathcal{M}_\odot<12$, or $0.27<\log\mathcal{M}<1.08$) gives the adopted slope of -1.37 ± 0.14. The derived slope is heavily dependent upon which mass range is chosen for the power-law fit. In NGC 457, which shows substantial structure in the luminosity/mass function, a power law may not be a useful characterization of the IMF.

3.9 NGC 436

The luminosity function [Fig. 10(a)] for NGC 436 (age 42 Myr) was constructed using field region 4. The apparent distance modulus of NGC 457, $(m-M)_V=14.10$, coupled with a completeness limit in the photometry at $V\sim 19$, results in the luminosity function being complete to $M_V\sim 5$. Although a slight dip at about $M_V\sim 3$ is seen in the luminosity function, it is not statistically significant on its own, although it occurs in the part of the luminosity function where dips are seen in several other clusters. A gradual drop in the luminosity function occurs at $M_V=5$ although this is close to the completeness limit of the photometry.

The mass function for the cluster is shown in Fig. 10(b). A power-law fit to the region ($1.2<\mathcal{M}/\mathcal{M}_\odot<5.2$, or $0.07<\log\mathcal{M}<0.70$) gives a slope -0.38 ± 0.15, a remarkably flat value. Extending the power-law fit to the highest mass of $12\mathcal{M}_\odot$ (which is, however, likely to be an evolved mass) results in a slope of -0.84 ± 0.16. The cluster is old enough that dynamical evolution would likely have occurred, resulting in the preferential loss of low mass stars. The small field of view (6.6×6.6 arcmin) likely

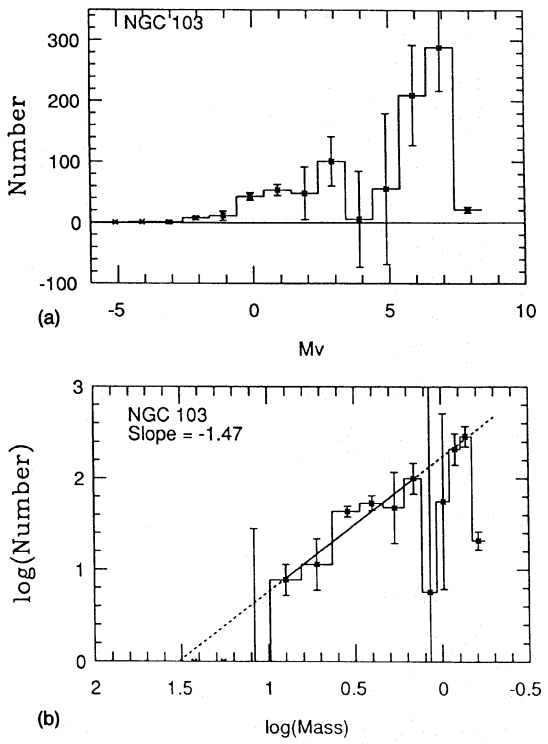

FIG. 11. (a) Luminosity function for NGC 103. (b) Mass function for NGC 103. Solid line indicates region over which the least-squares fit was made, omitting the point in the dip, yielding a slope of -1.47 for the mass function. Dashed line (long dashes) is the fit over the entire region where the photometry is complete, with the faint end of the mass function, beyond the dip, consistent with the power-law fit.

would not include all of the low mass stars, suggesting that the flat IMF could, at least in part, be explained by dynamical evolution of the cluster.

3.10 Berkeley 62

Field region data appropriate for the construction of the luminosity and mass functions of Be 62 (age 10 Myr) were not obtained. The CMD (Paper I), however, shows a possible gap in the main sequence between $12.5 < V < 13.5$ ($-2 < M_V < -1$), or $5 < \mathcal{M}/\mathcal{M}_\odot < 8$. The probability of finding a gap of a factor of 1.6 times in mass, with $N=6$ stars above the gap, and assuming a power-law IMF with slope $\Gamma = -1.35$, is 0.02 using Eq. (2) (from Scalo 1986).

3.11 NGC 103

The combined photometry from field regions 2, 3, and 4 was used as the field region for NGC 103 (age 20 Myr). Although the field regions are located far from the cluster ($\sim 15°$), the distribution of field stars in the CMD of the cluster field appears to be similar to that in the field regions, suggesting it is possible to use the field region data for the construction of the cluster luminosity function. It should be stressed, however, that the field region data are not ideal, being located so far from the cluster.

The longer integration times for this cluster (12 min in V, 15 min in B) give a fainter completeness limit, estimated to be $V \sim 20.5$, which when coupled with the apparent distance modulus of $(m-M)_V = 14.61$, results in the derived luminosity function being complete to $M_V \sim 6$. The luminosity function is shown in Fig. 11(a), where a rise is found to $M_V = 7$ ($V \sim 21.5$), but with a pronounced dip occurring at $M_V = 4$. The steady rise to $V \sim 21.5$ indicates that the assumption of completeness to $V \sim 20.5$ is likely a conservative one.

The mass function is shown in Fig. 11(b), where a power-law fit to the mass range ($1.4 < \mathcal{M}/\mathcal{M}_\odot < 7.9$, or $0.16 < \log \mathcal{M} < 0.90$) gives a slope of -1.47 ± 0.23. Extrapolation of this power law to the lower masses, beyond, the dip shows that the power law fits the mass function to at least $0.72\mathcal{M}_\odot$.

There is also an indication, although slight, that a dip is present in the luminosity function at $M_V = 2$ [Fig. 11(a)]. The statistical significance of the dip, as indicated by the error bars, is quite low although the location of the dip corresponds to a gap in the CMD and two-color diagram (TCD) of Fig. 12, showing only those stars within 1.4 arcmin of the cluster center. These diagrams improve the contrast of cluster stars over field stars compared to the full CMD and TCD (Paper 1), although the gap is also apparent in those diagrams. The gap in the CMDs occurs at $V = 16.5$–17.0, corresponding to $M_V = 2$–2.5, as is seen in the luminosity function.

The detection of structure in both the CMD and in the luminosity function is encouraging since it shows that the statistically derived luminosity functions do reveal real features.

3.12 NGC 7790

NGC 7790 is a much older cluster (71 Myr) than the other clusters in our sample. As in the case of NGC 103, a combination of field regions 2, 3, and 4 was used to construct the luminosity and mass functions, which are shown in Fig. 13(a). Nonphotometric conditions necessitated shorter exposure times for the NGC 7790 images (5 min in both V and B), resulting in photometry that is complete to only $V \sim 18$ which, with the apparent distance modulus of $(m-M)_V = 14.56$, results in the luminosity function being complete to $M_V \sim 3.5$.

A power-law fit to the mass function [Fig. 13(b)] over the mass range which is essentially unevolved and completely sampled ($1.4 < \mathcal{M}/\mathcal{M}_\odot < 7.9$, or $0.16 < \log \mathcal{M} < 0.90$) gives a slope of -1.64 ± 0.16. NGC 7790 is the oldest of the eight clusters for which luminosity and mass functions have been calculated, but has the second steepest IMF. NGC 436, with a 42 Myr age, has the shallowest IMF. As discussed in Sec. *3.9*, the shallow mass function for NGC 436 may be a result of its dynamical evolution and the smaller field that was observed around it.

In order to test whether the mass function for NGC 7790 is significantly affected by incomplete sampling of low mass stars as a result of dynamical evolution, the mass function was calculated at 0.57 arcmin annuli around the

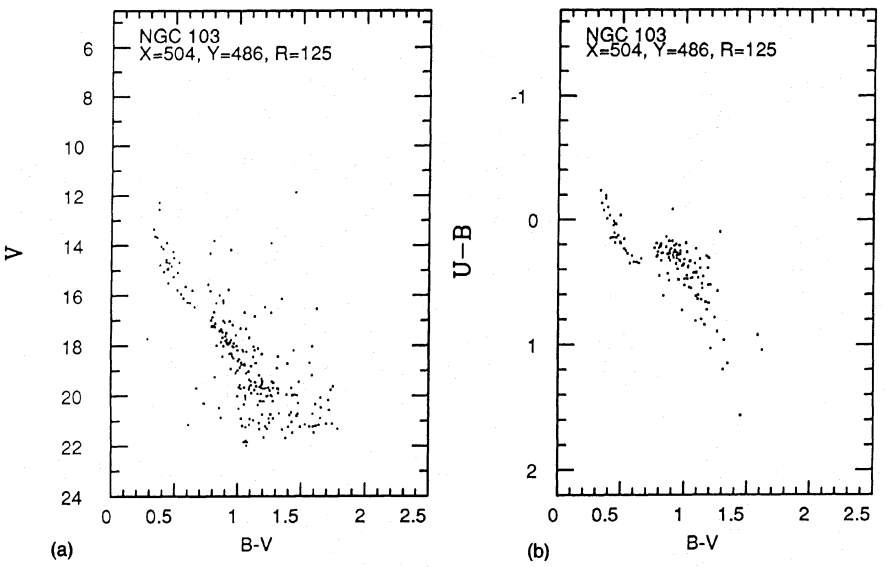

FIG. 12. (a) CMD for stars within 1.4 arcmin of NGC 103. (b) TCD for stars within 1.4 arcmin of NGC 103.

cluster center. If low mass stars are preferentially located in the outer region of the cluster, the slope (Γ) of the mass function should increase with greater radii, and reach a constant level as the cluster "boundary" is reached. Table 5 presents the result of this test, with the slope (Γ) leveling off to a constant value at a radius of $\sim$4.0 arcmin, which is very near the derived full radius of 3.6 arcmin, and is well within the boundaries of the observed field. The uncertainty in the slope, σ, is given in column 3 of Table 5. The mass function of NGC 7790, although a function of radius from the cluster center, has been sampled extensively enough that dynamical evolution should not appreciably affect the derived slope.

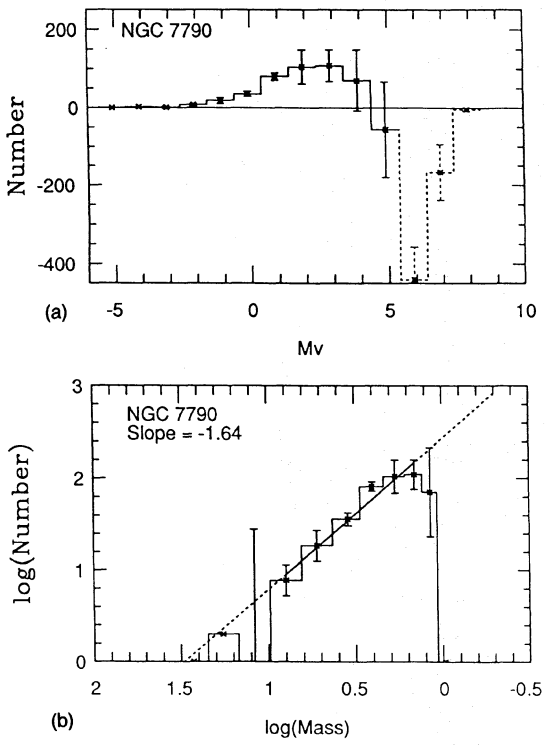

FIG. 13. (a) Luminosity function for NGC 7790. (b) Mass function for NGC 7790. Solid line indicates region over which the least-squares fit was made, yielding a slope of -1.64 for the mass function.

4. DISCUSSION

The conversion of the observed luminosity functions to mass functions requires the assumption that the stars are main-sequence objects. No evolutionary corrections were made despite evidence that at least some of the clusters show $\sim$10 Myr age spreads of the stars within them which is comparable to the ages of the clusters themselves (Paper I). The youth of the clusters also means that the lower mass stars will be pre-main-sequence objects. With the exceptions of NGC 436 and NGC 7790 (42 and 71 Myr old, respectively), the clusters for which luminosity functions have been calculated are $\sim$20–25 Myr old. For this age,

TABLE 5. NGC 7790: Variation of Γ with radius.

Radius (arcmin)	Γ	σ
1.1	-0.94	0.16
1.7	-1.14	0.17
2.3	-1.23	0.21
2.8	-1.40	0.16
3.4	-1.54	0.15
4.0	-1.63	0.19
4.5	-1.74	0.20
5.1	-1.65	0.18
Full	-1.64	0.16

TABLE 6. Derived mass functions.

Name	Slope (Γ)	σ_Γ	Intercept (b)	σ_b	Mass range high,low	Log(mass) range high,low
NGC 663	−1.06	0.05	2.59	0.03	12,1.4	1.08,0.16
NGC 659	−1.14	0.17	1.84	0.14	18,1.9	1.26,0.27
Tr 1	−1.41	0.24	1.76	0.12	7.9,1.2	0.90,0.07
NGC 581	−1.78	0.05	2.53	0.03	12,0.98	1.08,−0.01
NGC 457	−1.37	0.14	2.27	0.10	12,1.9	1.08,0.27
NGC 436	−0.38	0.15	1.52	0.06	5.2,1.2	0.72,0.07
NGC 103	−1.47	0.23	2.23	0.13	7.9,1.4	0.90,0.16
NGC 7790	−1.64	0.16	2.43	0.09	7.9,1.4	0.90,0.16

stars with masses less than about 1.2$\mathcal{M}_\odot$ will not yet have reached the main sequence (Stahler 1983), and the mass–luminosity relation of Scalo (1986) would be inappropriate. The range over which the mass function is calculated, however, is at or above this mass in all cases, except for NGC 581, where a lower mass of 0.98 was used. The use of the Scalo (1986) mass–luminosity relation close to, but below, this mass (e.g., in NGC 581, or with the extrapolation to lower masses in NGC 103), does not result in significant errors since the evolution of these PMS objects is essentially horizontal in the CMD (Stahler 1983).

The ages of the clusters are such that dynamical evolution will have had time to occur (Lada *et al.* 1984). The average radius determined for the clusters in this study is 3.38 pc (Paper I). Using the positions and magnitudes [converted into masses by the Scalo (1986) mass–luminosity relation] of stars in the Pleiades (Stauffer 1993) we find that ~75% of the mass of the Pleiades is contained within a similar radius. The Pleiades, with an age of 50–70 Myr (Stauffer 1982), is similar in age to NGC 7790 but is significantly older than the remainder of clusters we have studied, and therefore will have undergone more dynamical evolution. This, coupled with the fact that stars outside of the derived radii of the clusters were always used when constructing the luminosity functions (since the complete set of photometry for each cluster extended beyond the derived radii, see Paper I), means that our luminosity and mass functions should sample at least 75% of the mass of the clusters, on average.

Kroupa *et al.* (1991) have studied the effects of unresolved binaries on the form of the IMF, where they modeled systems with components randomly drawn from the same mass function. Luminosity functions with unresolved binaries, while substantially different from those with only single stars at faint magnitudes ($M_V > 7$–8), are essentially identical at the brighter magnitudes accessible in this study [see also Kroupa *et al.* (1992) for a discussion of binaries and the IMF of NGC 2362]. The effects of binaries on the derived mass functions of the program clusters are not significant and are neglected in the interpretation of the data.

A summary of the derived mass functions of the eight clusters is presented in Table 6, giving the slope of the mass function (Γ), the uncertainty in the slope (σ_Γ), the intercept (b), the uncertainty in the intercept (σ_b), the mass range over which the power law was fit, and the corresponding logarithmic mass range.

4.1 Is There a Single Open Cluster IMF?

Although variations do exist in the IMFs of young open clusters, it is interesting to determine the "average IMF" of young open clusters, which in this study, is the average of seven clusters (NGC 436 was omitted due to the likelihood that low mass stars have had time to escape, or form a halo which was not observed). Each cluster luminosity (and hence mass) function was normalized to have the same

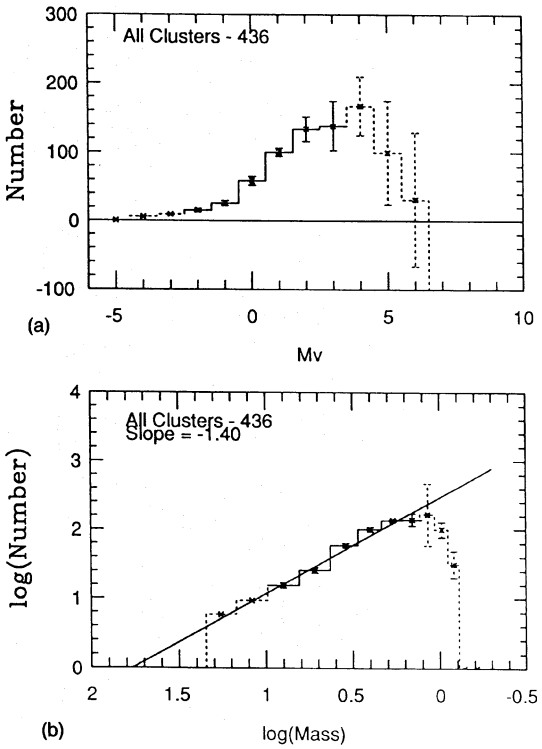

FIG. 14. (a) Luminosity function for all clusters, excluding NGC 436. Solid portion of the histogram is the region over which all luminosity functions are complete. (b) Mass function for all clusters, excluding NGC 436. Solid portion of the histogram is the region over which all mass functions are complete. Solid line indicates region over which the least-squares fit was made, yielding a slope of −1.40 for the average mass function.

number of stars at $M_V=1$. The resulting average cluster luminosity function is shown in Fig. 14, where the solid line represents the region of the luminosity function over which all clusters have been completely sampled, and where evolutionary effects have not occurred in the stars. This occurs over the range $-2<M_V<3$, corresponding to a mass range of $1.4<\mathcal{M}/\mathcal{M}_\odot<7.9$, or $0.16<\log \mathcal{M}<0.90$.

A steady rise is seen through the region of completeness, with a flattenining at $M_V=3$, due to the dip in the luminosity functions seen in several clusters at $M_V=2$–3. A power-law fit to the range of completeness gives a slope of -1.40 ± 0.13 over the mass range $1.4<\mathcal{M}/\mathcal{M}_\odot<7.9$, in good agreement with the Salpeter (1955) slope of -1.35. The average deviation of the individual slopes from the average slope is $\Delta_\Gamma=0.19$, with a dispersion of the mean equal to 0.15. The only clusters that show a significant deviation from this average slope are NGC 663 with a shallow IMF, and NGC 581 with a steep slope. Both of these clusters are quite populous and nearly identical in age and physical size. Both clusters were extensively sampled and the differences in their IMFs are likely to be real.

The slope of the "cluster IMF" is, on average, remarkably similar to the Salpeter (1955) IMF over the mass range $1.4<\mathcal{M}/\mathcal{M}_\odot<7.9$, with a slope of -1.40 ± 0.13, indicating that a power-law IMF, with a single slope, is a useful characterization of the stellar mass distribution over this mass range, although deviations do occur.

4.2 Is There Structure in the Luminosity Functions?

Wilner & Lada (1991), based upon their determination of the luminosity function of NGC 2362, have suggested the presence of a dip in its luminosity function at magnitudes corresponding to mid-A to mid-F main-sequence stars, with $1.5<M_V<3.5$ ($1.3<\mathcal{M}/\mathcal{M}_\odot<2.0$, or $0.1<\log(\text{mass})<0.3$). They note that a similar gap is also observed in the luminosity function of NGC 3293 (Herbst & Miller 1983), which is roughly the same age as NGC 2362 (7 Myr according to Mermilliod & Maeder 1986; an age spread from 7 to 22 Myr according to Kroupa *et al.* 1992). As pointed out by Wilner & Lada (1991), it is difficult to assess the significance of the dip due to the limited statistical sample. They do, however, argue that its occurrence in two clusters is suggestive of a physical cause.

Stahler & Fletcher (1991) have calculated models of the time evolution of the IMF from 10^5 to 10^8 yr, including protostars, PMS stars, and main-sequence stars. At early stages in the formation of a cluster (1 Myr), the luminosity function of a cluster exhibits a high luminosity peak [$\log(L/L_\odot)=1.5$] due to protostellar accretion. A large gap in the luminosity function toward the faint end of this peak results from an abrubt change in the mass–luminosity relation for PMS stars at this $2\mathcal{M}_\odot$ mass range (Stahler 1989). As accretion ceases, the star follows a PMS evolutionary track, until it reaches the main sequence. Around 5–10 Myr the protostellar peak has essentially vanished, but a broad, shallow dip in the luminosity function exists from $0<\log(L/L_\odot)<1.5$. This dip persists to 20 Myr, but moves to lower luminosities [$-0.1<\log(L/L_\odot)<0.5$]. By 50 Myr the luminosity function approaches a power law distribution.

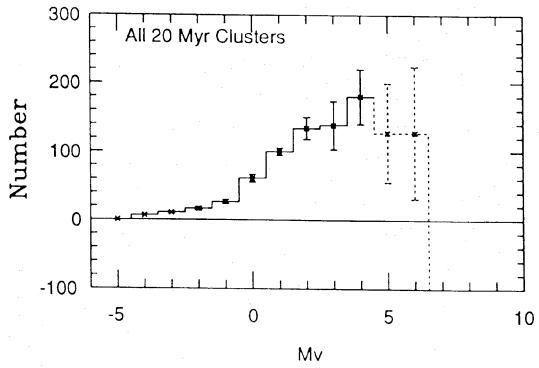

FIG. 15. (a) Luminosity function for all clusters with an age of ~20 Myr (all except NGC 436 and NGC 7790). Solid portion of the histogram is the region over which all luminosity functions are complete.

The dip in the luminosity function observed by Wilner & Lada (1991) and Herbst & Miller (1983) occurs for $1.5<M_V<3.5$ or $0.5<\log(L/L_\odot)<1.3$ using the calibration of M_V and $\log(L/L_\odot)$ from Schmidt-Kaler (1982), precisely where the calculations of Stahler & Fletcher (1991) indicate a dip should be present in a cluster of 10 Myr.

The average age of the clusters for which our luminosity functions have been obtained, excluding NGC 436 and NGC 7790, is 22.5 ± 4 Myr, for which the Stahler & Fletcher (1991) model suggests a dip should be present for $-0.1<\log(L/L_\odot)<0.5$, or $3.5<M_V<5$. Figure 15 shows the combined luminosity function for the ~20 Myr old clusters, where within the error bars, there is no apparent structure. Although a large dip over this magnitude range is apparent in NGC 103 and NGC 457, the complete absence of any significant features in other clusters of similar age (NGC 581 and NGC 663) indicates that, while gaps may be common features in luminosity functions, their significance is difficult to determine.

4.3 Gaps at the High Mass End of the IMF

As suggested by Scalo (1986), consideration of the IMF as a probability distribution means that gaps in the main sequence are possible, with a probability dependent upon the number of stars found at the high mass end of the gap [see Eq. (2)]. Several clusters have suggestions of such gaps; Be 7 (<4 Myr old) with a gap from $3.0<\mathcal{M}/\mathcal{M}_\odot<4$, NGC 637 (<4 Myr old) with a gap from $8<\mathcal{M}/\mathcal{M}_\odot<12$, and Be 62 (10 Myr old) with a gap from $5<\mathcal{M}/\mathcal{M}_\odot<8$. According to the relation given by Scalo (1986), given in Eq. (2), the probabilities of finding such gaps, using a slope of -1.35 for the IMF, are 0.07 -0.16, 0.02, and 0.02, respectively.

It is difficult to assess the significance of these gaps. Just by chance, given the small number of high mass stars, gaps should be expected in a few clusters. The low probabilities

of finding random statistical fluctuations this large, coupled with the fact that only the very youngest of the clusters have such high/intermediate mass gaps, may, however, suggest a physical cause. Although such gaps have also been seen in a number of other young open clusters (Mermilliod 1976), the small number of high mass stars, and the resulting poor statistics involved, must be carefully weighed when making assertions about such features. This is true, in general, when discussing gaps and dips in the luminosity and mass functions of clusters.

5. SUMMARY

Luminosity and mass functions have been calculated for eight open clusters, using statistical subtractions of field star data to correct for membership uncertainties. The slope of the average mass function for seven of these clusters is $\Gamma = -1.40 \pm 0.13$ over the mass range $1.4 < \mathcal{M}/\mathcal{M}_{\odot} < 7.9$, quite close to the Salpeter (1955) value of -1.35. Significant variations from this average value are found in only two clusters, NGC 581 and NGC 663. The 41 Myr cluster NGC 436 was found to have a very shallow mass function, most likely resulting from undercounting of the low mass stars due to dynamical evolution of the cluster.

No convincing evidence for structure, from $2 < M_V < 4$, is found in the average luminosity function for $\sim$20 Myr clusters, although it may be expected as a result of the effects of stellar evolution (Stahler & Fletcher 1991). Variations do occur, however, with the luminosity functions of NGC 581 and NGC 663 exhibiting a steady rise over this range, while NGC 103, with the same age, shows a large gap. A sharp drop, well within the completeness limit, in the luminosity and mass function of NGC 457 is found. Gaps at the higher end of the mass function of the youngest clusters are also found, although their significance is difficult to determine.

The authors would like to thank the referee, Dr. John Stauffer, for his useful comments and suggestions. This research was part of Randy Phelps' Ph.D. thesis work at Boston University.

REFERENCES

Herbst, W., & Miller, D. P. 1983, AJ, 87, 1478
Hodapp, K.-W., & Rayner, J. 1991, AJ, 102, 1108
Janes, K., & Heasley, J. 1993, PASP, 105, 527
Jones, B. F., & Stauffer, J. R. 1991, AJ, 102, 1080
Jones, B. F., & Stauffer, J. R. 1982, AJ, 87, 1507
Kroupa, P., Gilmore, G., & Tout, C. A. 1992, AJ, 103, 1602
Kroupa, P., Gilmore, G., & Tout, C. A. 1991, MNRAS, 251, 293
Lada, C. J., DePoy, D. L., Merrill, K. M., & Gatley, I. 1991, ApJ, 374, 539
Lada, C. J., & Lada, E. 1991, in The Formation and Evolution of Star Clusters, PASP Conference Series, edited by K. A. Janes (ASP, San Francisco), p. 3
Lada, C. J., Margulis, M., & Dearborn, D. 1984, ApJ, 285, 141
Larson, R. B. 1986, MNRAS, 218, 409
Lyngå, G. 1987, Catalog of Open Cluster Data (Observatoire de Strasbourg, Centre de Données Stellaires)
McCaughrean, M., Rayner, J., & Zinnecker, H. 1991, MSAIt, 62, 715
Mermilliod, J. C. 1976, A&A, 53, 289
Mermilliod, J. C., & Maeder, A. 1986, A&A, 158, 44
Mezger, P. G., & Smith, L. F. 1977, in Star Formation, IAU Symposium No. 75, edited by T. de Jong and A. Maeder (Reidel, Dordrecht), p. 133
Miller, G. E., & Scalo, J. M. 1979, ApJS, 41, 513
Phelps, R. L., & Janes, K. A. 1993, ApJS (in press)
Reid, N. 1992, MNRAS, 257, 257
Salpeter, E. E. 1955, ApJ, 121, 161
Scalo, J. 1986, Fund. Cos. Phys., 11, 144
Schmidt-Kaler, T. 1982, Landolt–Bornstein VI, Vol. 2b (Springer, Berlin)
Stahler, S. W. 1989, ApJ, 347, 950
Stahler, S. W. 1983, ApJ, 274, 822
Stahler, S. W., & Fletcher, A. B. 1991, MSAIt, 62, 767
Stauffer, J. 1993, personal communication
Stauffer, J., Klemola, A., Prosser, C., & Probst, R. 1991, AJ, 101, 980
Stetson, P. 1987, PASP, 99, 191
Tinsley, B. 1980, Fund. Cos. Phys., 5, 287
van den Bergh, S., & Sher, D. 1960, Publ. David Dunlop Obs., 2, 203
Wilking, B. A., Lada, C. J., & Young, E. T. 1989, ApJ, 340, 823
Wilner, D. J., & Lada, C. J. 1991, AJ, 102, 1050
Zinnecker, H. 1986, in Highlights in Astronomy, 7, edited by J.-P. Swings (Reidel, Dordrecht)
Zinnecker, H., & McCaughrean, M. 1991, MSAIt, 62, 761